HHS Public Access

Author manuscript

Free Radic Biol Med. Author manuscript; available in PMC 2018 April 12.

Published in final edited form as:

Free Radic Biol Med. 2018 March ; 117: 180–190. doi:10.1016/j.freeradbiomed.2018.02.006.

Mitochondrial protein *S*-nitrosation protects against ischemia reperfusion-induced denervation at neuromuscular junction in skeletal muscle

Rebecca J. Wilson[d,f], **Joshua C. Drake**[f], **Di Cui**[f], **Bevan M. Lewellen**[f], **Carleigh C. Fisher**[f], **Mei Zhang**[a,f], **David F. Kashatus**[e], **Lisa A. Palmer**[a], **Michael P. Murphy**[g], **Zhen Yan**[a,b,c,f,*]

[a]Departments of Medicine, University of Virginia School of Medicine, Charlottesville, VA 22908, USA

[b]Departments of Pharmacology, University of Virginia School of Medicine, Charlottesville, VA 22908, USA

[c]Departments of Molecular Physiology and Biological Physics, University of Virginia School of Medicine, Charlottesville, VA 22908, USA

[d]Departments of Biochemistry and Molecular Genetics, University of Virginia School of Medicine, Charlottesville, VA 22908, USA

[e]Departments of Microbiology, Immunology, and Cancer Biology, University of Virginia School of Medicine, Charlottesville, VA 22908, USA

[f]Center for Skeletal Muscle Research at Robert M. Berne Cardiovascular Research Center, University of Virginia School of Medicine, Charlottesville, VA 22908, USA

[g]MRC Mitochondrial Biology Unit, University of Cambridge, Cambridge, UK

Abstract

Deterioration of neuromuscular junction (NMJ) integrity and function is causal to muscle atrophy and frailty, ultimately hindering quality of life and increasing the risk of death. In particular, NMJ is vulnerable to ischemia reperfusion (IR) injury when blood flow is restricted followed by restoration. However, little is known about the underlying mechanism(s) and hence the lack of effective interventions. New evidence suggests that mitochondrial oxidative stress plays a causal role in IR injury, which can be precluded by enhancing mitochondrial protein *S*-nitrosation (SNO). To elucidate the role of IR and mitochondrial protein SNO in skeletal muscle, we utilized a clinically relevant model and showed that IR resulted in significant muscle and motor nerve

*Corresponding author at: Center for Skeletal Muscle Research at Robert M. Berne Cardiovascular Research Center, University of Virginia School of Medicine, 409 Lane Road, MR4-6031A, Charlottesville, VA 22908, USA. zhen.yan@virginia.edu (Z. Yan).

Conflicts of interest

The authors have no conflict of interest to declare.

Author contributions

R.J.W. designed the study, conducted experiments, analyzed and interpreted data, and wrote the manuscript. J.C.D. designed the study, interpreted data, and edited the manuscript, D.C., B.M.L., C.C.F., and M.Z. performed experiments, analyzed data, and provided technical support, D.K. interpreted data, and edited the manuscript, M.P.M. designed the study, interpreted data, edited the manuscript, Z.Y. designed the study, interpreted data, and wrote the manuscript.

injuries with evidence of elevated muscle creatine kinase in the serum, denervation at NMJ, myofiber degeneration and regeneration, as well as muscle atrophy. Interestingly, we observed that neuromuscular transmission improved prior to muscle recovery, suggesting the importance of the motor nerve in muscle functional recovery. Injection of a mitochondria-targeted *S*-nitrosation enhancing agent, MitoSNO, into ischemic muscle prior to reperfusion reduced mitochondrial oxidative stress in the motor nerve and NMJ, attenuated denervation at NMJ, and resulted in accelerated functional recovery of the muscle. These findings demonstrate that enhancing mitochondrial protein SNO protects against IR-induced denervation at NMJ in skeletal muscle and accelerates functional regeneration. This could be an efficacious intervention for protecting neuromuscular injury under the condition of IR and other related pathological conditions.

Keywords

Ischemia reperfusion; *S*-nitrosation; Mitochondria; Oxidative stress; Skeletal muscle; Motor nerve; Neuromuscular junction

1. Introduction

Neuromuscular junction (NMJ) is a unique microdomain where a motor neuron and skeletal muscle fiber interface to coordinate voluntary muscle contractions. Conditions in which neuromuscular function is compromised, such as amyotrophic lateral sclerosis [1], aging [2], muscular dystrophies [3] and traumatic injuries [4], are often characterized by deterioration of NMJ. In particular, following certain types of surgeries or as a first response to traumatic injury, in which a tourniquet is used to control blood flow, skeletal muscle and motor nerves are often damaged by ischemia reperfusion (IR), caused by interruption in tissue perfusion and subsequent restoration of blood flow. In addition to muscle weakness and atrophy [5,6], IR injury can cause irreversible nerve and NMJ damage [7,8], all of which hinder functional recovery of the affected skeletal muscle. However, we know little about the underlying mechanism(s) of IR-induced neuromuscular damage, and hence there is currently no reliable and effective intervention [9–11].

Mitochondria are enriched on the pre- and post-synaptic sides of NMJ [12,13] and are essential for NMJ development, stability, and neurotransmission [14–16]. Perturbations that alter mitochondrial energy production, Ca^{2+} buffering, or increase oxidative stress, play a causal role in NMJ degradation and neuromuscular dysfunction [1,17]. In the context of IR injury, excessive generation of mitochondria-derived reactive oxygen species (mtROS), which leads to mitochondrial oxidative stress, are considered central to the initiation and exacerbation of IR pathology [18,19]. Mitochondria transfer electrons through the electron transport system (ETS) to drive the formation of adenosine triphosphate (ATP), which serves as chemical energy storage used directly for all biological processes [20]. During normal mitochondrial oxidative respiration, a small percentage of electrons escape the ETS and form superoxide [21], which is rapidly scavenged and detoxified by the resident antioxidant enzymes and molecules [22,23]. During ischemia, tissue oxygen supply is discontinued and mitochondrial oxidative respiration suspended [24]. Depending on the duration of ischemia, there will be insufficient production of ATP and accumulation of ADP as well as other

intermediate metabolites and reducing equivalents, such as NADPH and succinate [25,26]. Upon reperfusion, these metabolic buildups cause a surge of mtROS from the ETS [21,27]. When the production of mtROS exceeds the capacity of the mitochondrial antioxidant defense system, it results in oxidization of cellular components (e.g. DNA, protein and lipid, etc.), causing tissue damage and dysfunction and/or cell death [28,29]. Furthermore, mtROS may further damage mitochondrial structure and impair function [30], leading to a vicious cycle [29,30]. Therefore, prevention of mtROS production or neutralization of the reactive molecules may prove be the most efficacious intervention against IR injury.

Nitric oxide (NO) and its derivatives have been found to interact with the mitochondrial proteome, modulating respiration and providing cytoprotective effects [33] in the context of IR injury. In particular, mitochondrial protein *S*-nitrosation (SNO) reversibly inhibits mitochondrial respiration, prevents mtROS production by reverse electron transfer (RET) at complex I of the ETS [25], and shields protein cysteine residues from irreversible oxidation [34,35]. Enhancement of mitochondrial SNO either by ischemic preconditioning [36] or treatment with NO donor [37–40] has been found to be protective in models of myocardial infarction; however, whether such strategies are applicable for conditions of neuromuscular injuries in skeletal muscle and how enhanced mitochondrial SNO might lead to the protection are unknown. In the present study, we utilized a clinically relevant model of tourniquet-induced IR injury in mouse hindlimb to test whether pharmacological augmentation of mitochondrial SNO could preserve muscle and/or motor nerve structural integrity and function with improved recovery from IR. We employed the state-of-the-art mitochondrial reporter technology to elucidate the underlying mechanism(s) of the pathology of IR injury with a focus on mitochondrial oxidative stress in both adult skeletal myofibers and motor nerves.

2. Results

2.1. Tourniquet-induced IR in skeletal muscle causes both nerve and muscle damages

To determine the impact of IR injury on nerve and muscle function, we applied a tourniquet above the right femur of a mouse to induce ischemia for 1 h, a duration compatible with the clinical guidelines, followed by removal of the tourniquet to initiate reperfusion [41]. We performed a 28-day longitudinal study, in which we measured the maximal tetanic force production of the planter flexors in vivo via nerve stimulation or direct muscle stimulation. These protocols provide insight into neuromuscular transmission and force generating capacity of the muscle, respectively [9,42]. In un-injured mice (sham), force production resulting from nerve and muscle stimulations was indistinguishable (Fig. 1a). However, at day 7 following IR injury, forces generated by nerve and muscle stimulations were reduced by 80% and 50%, respectively, compared to the sham control (Fig. 1a and Supplemental Table 1). The additional deficit in force production via nerve stimulation is indicative of impaired neuromuscular transmission. At day 14 post-injury, nerve stimulation-elicited force production became equal to that produced by muscle stimulation while the latter had not changed. By day 28, force production by muscle and nerve stimulation significantly increased and had recovered to the level of sham control mice when normalized to muscle weight (Fig. 1b). In a parallel, terminal experiment over the same time course, we confirmed

that reduction in force between days 7 and 14 even when we normalized the force by muscle mass, suggesting its independency of muscle atrophy (Supplemental Fig. 1). These findings demonstrate that IR causes injury to nerve and muscle, and neuromuscular transmission recovers prior to functional recovery of muscle.

To assess muscle injury, we measured serum creatine kinase (CK) activity, a marker of muscle damage [43,44]. CK was elevated 4-fold between 3 and 12 h post-IR compared to the sham control mice before returning to the baseline after 1 day (Fig. 1c). This initial, transient increase in CK activity suggests that a single damaging event to the muscles. Muscle damage was further confirmed by reduced gastrocnemius wet weight to 40% of the sham control at day 14 (Fig. 1d). Furthermore, histological analysis by hematoxylin and eosin (H&E) staining revealed a gradual increase of centrally located myonuclei, a marker of muscle regeneration [45], over the 28-day experimental period (Fig. 1e), suggesting ongoing regeneration.

Finally, we examined innervation at neuromuscular junctions (NMJ) in the middle portion of the plantaris muscle. Muscle contraction begins at NMJ where neurotransmitter acetylcholine is released by the motor nerve (pre-synaptic) and binds to its receptor on the muscle (post-synaptic), initiating a cascade of events that lead to contraction and force generation [46]. Impairment of structure and/or function on either pre- or post-synaptic side of NMJ will impair muscle contraction [47]. We assessed NMJ innervation by measuring the overlap of immunoreactivity of the presynaptic markers β-III tubulin (Tuj1) and synaptic vesicle proteins (SV2) with the post-synaptic acetylcholine receptor (AchR) detected by α-bungarotoxin (α-BTX). We found a significant reduction in Tuj1/SV2-α-BTX overlap at 3 h following IR injury compared to the sham control. This was followed by a partial recovery at day 28 (Fig. 1f). Importantly, the reduction in Tuj1/SV2-α-BTX overlap was due to a loss of the immunoreactivity of the pre-synaptic structures, indicative of NMJ denervation. These data suggest that 1-h tourniquet application followed by reperfusion in mouse hindlimb leads to both muscle and nerve injury, and temporal findings also raise the possibility that functional recovery of skeletal muscle may, at least in part, depend on motor nerve recovery.

2.2. Ischemia-reperfusion causes mitochondrial oxidative stress in skeletal muscle, motor nerve, and NMJ

Since mtROS production is considered central to IR injury [18,19], we sought to determine whether tourniquet-induced IR causes mitochondrial oxidative stress within the neuromuscular system. To address this question we crossed *CAG-CAT-MitoTimer* mice with *CAG-CreER*^{T2} mice to obtain *MitoTimer* reporter mice with global inducible expression of *MitoTimer*, a novel redox-sensitive mitochondrial-targeted reporter gene [32,48,49]. We observed a significant increase in Mito-Timer red: green ratio in plantaris muscle (Fig. 2a) and sciatic nerve (Fig. 2b) 3 h following IR injury, emblematic of increased mitochondrial oxidative stress [32,48,49]. To assess the mitochondrial oxidative stress at NMJ we utilized α-BTX to identify NMJ and imaged areas in which MitoTimer and α-BTX overlapped (Fig. 2c). In accordance with electron microscopy studies that show an enrichment of mitochondria at NMJ [14], MitoTimer fluorescence was concentrated in a similar pattern

as α-BTX. Moreover, MitoTimer red: green ratio in this region was significantly greater 3 h following IR as compared to those in the sham control mice, providing the first quantitative measurement of oxidative stress in the mitochondria of NMJ in vivo. Clustering of MitoTimer with α-BTX was confirmed to be indicative of mitochondria at the NMJ using MitoTracker and α-BTX (Supplemental Fig. 2a and 2b). These findings demonstrate that IR causes mitochondrial oxidative stress in plantaris muscle, sciatic nerve and NMJ.

2.3. MitoSNO protects motor nerve function, leading to improved functional regeneration of skeletal muscle

Since mitochondrial SNO has been found to reversibly depress mitochondrial respiration, reduce mtROS generation and shield cysteine residues from oxidation [50], we investigated whether promoting mitochondrial SNO was sufficient to attenuate muscle and/or nerve damage. We administered saline, MitoSNO (a mitochondrial targeted *S*-nitrosothiol) or MitoNAP (the thiol precursor of MitoSNO for the non-SNO effects of MitoSNO) [39]. We confirmed that MitoSNO treatment had to be administrated prior to reperfusion to be effective (Supplemental Fig. 3a and 3b), consistent with the previous findings in the heart [38]. To determine the consequence of MitoSNO treatment following IR injury, we measured tetanic force production in vivo by muscle or nerve stimulation. At day 7 post-IR, force production via nerve stimulation was significantly greater in MitoSNO-treated muscles compared to MitoNAP- or saline-treated muscles (Fig. 3a), providing the first evidence of motor nerve. Ischemic-preconditioning has previously shown not effective in preventing neuromuscular dysfunction induced by IR [9,51]. Conversely, force production induced by direct muscle stimulation was reduced similarly in saline-, MitoNAP- and MitoSNO-treated hindlimb muscles compared to the sham control (Fig. 3a), suggesting an equal level of damages to the muscles under these conditions. At day 14 following injury, neuromuscular transmission had recovered in all groups, but MitoSNO-treated muscles generated significantly greater force, suggesting that MitoSNO treatment promotes functional regeneration of skeletal muscle following IR injury.

Next, we assessed muscle mass and found a similar reduction (~ 40%) in of gastrocnemius muscle wet weight in saline-, MitoNAP-, and MitoSNO-treated groups at 14 days post-IR compared to the sham control (Fig. 3b). Analysis of specific force revealed that specific force production in MitoSNO-treated muscle was indistinguishable from that of the sham control mice and was significantly higher than saline- and MitoNAP- treated muscles (Fig. 3c). These data indicate that MitoSNO treatment did not lead to a complete recovery of muscle mass but a complete recovery of muscle contractile function. Additionally, a lack of protection by administration of MitoNAP suggests that the protection by MitoSNO treatment is due to the presence of the NO moiety, which transnitrosates cysteine residues, rather than the antioxidant properties of the free thiol. Thus, we focused on MitoSNO in the subsequent experiments.

To confirm that intramuscular injection of MitoSNO during ischemia enhances mitochondrial protein SNO, we assessed mitochondrial protein SNO in grastrocnemius muscle and sciatic nerve using a biotin switch assay [52]. Levels of SNO of ETS complex I (NADH oxidoreductase 75 kDa subunit), II (Succinate dehydrogenase iron-sulfer subunit

B), III (Cytochrome c oxidase subunit 1), and V (ATP synthase subunit α) were significantly elevated compared to saline-treated muscle and the muscle of the sham control mice (Fig. 3d). Similar findings were obtained in sciatic nerve (Fig. 3e). These findings validate that intramuscularly injection of MitoSNO prior to reperfusion enhances SNO of mitochondrial proteins in skeletal muscle and motor nerve. Taken together, these findings suggest that MitoSNO treatment enhances SNO of mitochondrial proteins in both skeletal muscle and motor nerve, but effectively protects motor nerve and/or NMJ, leading to improved contractile function recovery post-IR injury.

2.4. MitoSNO treatment preserves innervation at NMJ following IR

To elucidate the impact of mitochondrial SNO on neuromuscular system, we subjected mice to IR with or without treatment with MitoSNO. Following IR, MitoSNO-treated muscle displayed a preserved overlap of α-BTX and Tuj1/SV2, suggesting protection against IR-induced NMJ denervation (Fig. 4a). This difference of innervation at NMJ between saline- and MitoSNO-treated muscles was maintained up to day 14 days post-IR. Additionally, the number of muscle fibers expressing neural cell adhesion molecule (Ncam), a marker of denervation [53], was increased at day 14 in saline-treatment muscles compared to the sham control, which was profoundly attenuated by MitoSNO treatment (Fig. 4b). These findings provide additional evidence for the protective effect of MitoSNO on NMJ from IR injury.

To assess the impact of MitoSNO treatment on muscle damage, we measured serum CK activity 3 h after IR and observed a 6-fold increase in serum CK activity (Fig. 4c) in Saline and MitoSNO groups compared with the Sham control group, suggesting a comparable degree of muscle damage. Histological analysis at day 14 revealed a significant increase in centralized nuclei in Saline group compared to the Sham control group, while MitoSNO treatment did not lead to a statistically significant reduction (Fig. 4d). Together, these data show that enhancing mitochondrial SNO by intramuscular injection of MitoSNO prior to reperfusion protects against IR-induced denervation at NMJ, which leads to overall improved functional recovery of muscle following IR.

2.5. MitoSNO treatment reduces IR-induced mitochondrial oxidative stress in the motor nerve

To determine whether reduction of mitochondrial oxidative stress underlies MitoSNO-mediated protection of the nerve function and innervation at NMJ, we subjected *MitoTimer* reporter mice to IR injury. IR injury led to a significant increase in MitoTimer red: green ratio in plantaris muscle (Fig. 5a), sciatic nerve (Fig. 5c) and NMJ (Fig. 5e) 3 h following IR, indicative of increased mitochondrial oxidative stress in both muscle fibers and motor nerve in the hindlimb. It is worthy noticing that mitochondrial oxidative stress has been reported under other conditions using this technology [32,49,54]. Treatment with MitoSNO, however, significantly attenuated the increase of MitoTimer red: green ratio in the sciatic nerve (Fig. 5c) and NMJ (Fig. 5e), but this effect in plantaris muscle was not statistically significant (Fig. 5a). Since the redox sensitive residue of MitoTimer is tyrosine 67 [55], which cannot undergo SNO, the reduction of MitoTimer red: green ratio in sciatic nerve following MitoSNO treatment is likely a consequence of reduced mtROS rather than direct shielding by SNO. We observed similar increases of lipid peroxidation induced by IR as

indicated by western blot analysis of 4-hydroxynonenal (4HNE), a marker of oxidative stress, in mitochondria isolated from plantaris muscle (Fig. 5b) and sciatic nerve (Fig. 5d), which was only reduced in sciatic nerve by MitoSNO treatment. Collectively, findings obtained by two independent assay systems indicate that MitoSNO treatment reduces IR-induced mitochondrial oxidative stress in the motor nerve leading to preservation of motor nerve/NMJ structure and neuromuscular transmission, facilitating functional rehabilitation of the muscle following IR injury.

3. Discussion

Impaired neuromuscular function, due to NMJ injury, is central to a number of diseases and traumas that affect muscle mass and force production, causing impairments in voluntary movement [1–4] While the mechanism(s) underlying deterioration in neuromuscular function and NMJ are still being uncovered, excessive generation of mtROS and consequential oxidative stress predominate [1,7,8,56] However, until now, there has been no therapeutics that directly target mitochondria to preserve neuromuscular integrity. In this study, we sought to elucidate the consequence(s) of IR injury on mitochondrial oxidative status and its impact on skeletal muscle and motor nerve function by employing a model directly relevant to usage of a tourniquet to control blood flow in certain clinical procedures in humans. We obtained functional, morphological, and biochemical evidence that recapitulates many of the consequences of IR injury observed in human skeletal muscle and motor nerves [7,57]. Furthermore, we found that treatment with MitoSNO, a mitochondria-targeted molecule that enhances SNO, protected motor nerves against IR injury and improved functional regeneration of the affected skeletal muscles. These findings identify intramuscular injection of MitoSNO as an effective intervention against IR injury and highlight the importance of nerve function on muscle recovery from IR injury.

Accumulation of oxidative stress within the NMJ mitochondria is thought to play a causal role in neuromuscular dysfunction [1]. Despite the recognized importance of mitochondria in neuromuscular function, technologies for assessment of mitochondrial morphology, function, and/or integrity at NMJ have been limited to electron microscopy [14,58], in vitro cell culture [59], or extrapolation of studies conducted in separate categories of nerve synapses using a variety of fluorescent probes [15]. These aforementioned approaches, however, do not provide insight into mitochondrial oxidative stress in NMJ in vivo. Here, we developed and utilized a novel transgenic mouse line, in which *MitoTimer,* a reporter gene for reporting mitochondrial oxidative stress, is inducibly expressed in all tissues of the body. We discovered that IR injury caused a significant increase of mitochondrial oxidative stress in the motor nerve and skeletal muscle. Taking advantage of fluorescently conjugated α-BTX, we ascertained MitoTimer signal hence mitochondrial oxidative stress at NMJ. Using this novel approach, we obtained clear evidence of increased mitochondrial oxidative stress in these discrete areas following IR injury. Together, these findings provide the first direct measurement of mitochondrial oxidative stress in NMJ.

Aberrant mtROS production upon rapid reactivation of mitochondrial respiration during reperfusion is critical for initiation and propagation IR injury [60]. Given the proximity to the primary site of mtROS production, mitochondrial macromolecules are especially

vulnerable to oxidative damage [61]. Accumulation of damaged mitochondrial proteins contributes to mitochondrial dysfunction, which effectively impairs tissue function and recovery [31]. Mitochondrial respiration can be regulated by redox-based protein modifications of cysteine residues. Particularly, enhanced SNO of proteins of ETS [27,38,62] and tri-carboxylic acid (TCA) cycle [24,36] have been found to elicit cyto-protective effects against IR injury. For example, studies of myocardial infarction reveal that SNO of Cys39 on the ND3 subunit of complex I by MitoSNO potently protects the heart from IR injury by slowing mitochondrial respiration and mtROS production during reperfusion [38,39]. Informed by this precedent, we asked whether treatment with MitoSNO could enhance SNO of ETS proteins and attenuate mitochondrial oxidative stress following IR injury. Our findings of enhanced SNO of the 75-kda subunit of complex I, a site of NADH oxidation, and complex II, the entry site of electrons from succinate to $FADH_2$ are consistent with the findings in cardiomyocytes [38,39]. Furthermore, administration of MitoSNO resulted in reduced mitochondrial oxidative stress in the sciatic nerve and preserved motor nerve function and NMJ innervation. Due to the scarce tissue availability, we could not ascertain whether MitoSNO treatment elicits the protection in motor nerve through SNO of Cys39 or other mitochondrial proteins that are susceptible to SNO in this study. It is worth noticing that sciatic nerve has greater induction of SNO of complex III than skeletal muscle in our model. However, there is currently no evidence that this change has any functional significance. We also acknowledge that this study has primarily focused on limited number of mitochondrial proteins. Enhanced SNO of other mitochondrial ETC proteins may contribute the protection. Future research should pinpoint the functional site of MitoSNO action in ETC and explore the possibility of SNO of other protein for the protection in motor nerve, which will aid in the development targeted therapeutics.

The mechanism by which enhancing mitochondrial protein SNO protects against IR is not entirely clear, particularly because ~ 1% of the cysteines of the mitochondrial proteome are available for SNO [39,62]. SNO has been found to shield critical cysteine thiols from irreversible oxidation and alter protein activity [36,50,62]. In addition to reversible modulation of enzyme activity, SNO shields cysteine residues from irreversible oxidation, which has been shown to protect proteins that are vulnerable to oxidant-mediated inactivation in the heart [67]. Thus, it is likely that MitoSNO mediated protection to the motor nerve is a synergistic effect of enhanced SNO of multiple ETS proteins, ultimately reducing mitochondrial oxidative stress and preserving mitochondrial function.

Loss of tissue viability and function are among the consequences of IR, and thus, attenuation of mitochondrial oxidative stress should curb these abnormalities. Indeed, we obtained substantial evidence that treatment with MitoSNO preserved nerve function following IR injury, as determined by the discrepancies between the forces elicited by nerve stimulation and direct muscle stimulation. This is most likely attributable to the aforementioned reduction in mitochondrial oxidative stress, which would maintain nerve function extending from the axon to the NMJ. Such reasoning is bolstered by other studies in models of diabetic neuropathy and ALS, in which administration of antioxidants or anti-oxidant gene mimetics attenuated loss of motor nerve conduction [68] and enhanced survival of motor neurons [69], respectively. However, additional studies are needed to parse the precise mechanism, by which mitochondrial oxidative stress abrogates nerve function upon IR injury.

Despite the potent protection of motor nerve by MitoSNO treatment, initial damage to skeletal muscle was not prevented. This lack of protection against skeletal muscle injury per se suggests that muscle damage may be mediated by a mechanism(s) independent of mtROS, such as ROS production from non-mitochondrial sources [70], and/or enhanced calpain activity [71]. Other studies have shown that necrotic and apoptotic cell death pathways in skeletal muscle are rapidly initiated during ischemia, and the degree of activation of cell death pathway is proportional to the duration of ischemia [72]. Thus, MitoSNO, which we administered immediately prior to reperfusion, would not likely affect damage occurred during ischemia. Importantly, our data that functional regeneration of muscles treated with MitoSNO exceeded that of the other groups suggests that the protection is mediated by a process other than direct protection against initial muscle injury.

Both the maintenance of muscle mass and contractile function under normal condition and the recovery following injury are highly affected by neuromuscular activity as well as neurotrophic factors. The influence of nerve on muscle functional regeneration are multifold, impacting muscle metabolism [73], sarcomeric organization [74] and muscle fibrillation [75]. Indeed, functional recovery of muscle following nerve crush injury has been previously shown to be accomplished, albeit gradually, only after neural input recovers [76]. We found that nerve function and NMJ innervation were preserved 7 days following treatment with MitoSNO when compared to MitoNAP- or saline-treated groups. Of great interest is the finding that MitoSNO treatment led to a more rapid recovery of contractile function without an appreciable reinnervation of the NMJ at day 14. These data suggest that the increase in force production between day 7 and 14 in MitoSNO-treated muscles is due to functional regeneration of the muscle. It is therefore likely that the accelerated improvement in muscle function is attributable to the preserved NMJ innervation and function during the initial phase of IR. Therefore, preservation of NMJ accelerates functional regeneration of skeletal muscle from IR injury.

In conclusion, our studies demonstrate that treatment with mitochondria-targeted *S*-nitrosythiol MitoSNO prior to reperfusion attenuates IR-induced denervation at NMJ and preserves neuromuscular function, which facilitate functional regeneration. Our findings highlight a here unto unappreciated role of the physiological consequences of enhanced SNO of mitochondrial proteins at NMJ and prove the feasibility of intramuscular injection of MitoSNO as an effective intervention against IR injury in skeletal muscle as an organ.

4. Material and methods

4.1. Animals

All animal procedures were conducted under the approval of the UVa animal care and use committee. Male C57Bl/6 between 9 and 12 weeks were obtained from Jackson Laboratory (Bar Harbor, ME). *MitoTimer* transgenic mice were generated by subcloning the *Mitotimer* coding region in an inducible expression vector downstream from LoxP-flanked chloramphenicol acetyltransferase (CAT) coding sequence [77] with a stop codon under the control of CMV early enhancer/chicken β actin (CAG) promoter [78]. We called this construct *pCAG-CAT-Mito-Timer,* which allows for inducible expression of MitoTimer following expression of the Cre recombinase. When we co-transfected *pCAG-*

CAT-MitoTimer with *pCMV-Cre*, an expression vector of Cre under the constitutively active *CMV* promoter, we observed MitoTimer expression while co-transfection with an empty vector, *pCI-neo*, showed no expression of MitoTimer). We then used the isolated DNA fragment containing the expression unit for pro-nuclei injection and a generated transgenic mouse line in C57BL/6 background, call *CAG-CAT-MitoTimer* mice. After we crossbred the *CAG-CAT-MitoTimer* mice with a global inducible Cre mouse line, *CAG-Cre-ER^{T2}*, we injected the adult global inducible MitoTimer mice (CAG-CAT-MitoTimer;*CAG-Cre-ER^{T2}*) with tamoxifen (40 mg/kg, i.p.) daily for 7 days and observed expression of MitoTimer in the skeletal muscle, heart, lung, liver, kidney and brain.

4.2. Ischemia-reperfusion injury

IR injury was induced by application of a 4.0-oz 1/8′ orthodontic rubberband (DENTSPLY GAC International Inc. 11-102-03) above the greater tronchanter of the femur using a McGivney Hemmrohidal Ligator as previously described [79]. The tourniquet was removed after 1 h to induce reperfusion. Experiments were performed at various time points ranging from 0 h (end of ischemia) to 28 days following IR.

4.3. Creatine kinase activity

Creatine kinase activity was measured following the manufacturer's instructions of a commercially available kit (Sigma Aldrich MAK116). Blood was collected from the tail, incubated at RT for 30 min then spun at 1,500 × *g* at 4 °C for 30 min. The clear portion was removed (serum) and the clot was discarded. Samples were aliquoted and stored at −80 °C until needed at which point they were thawed on ice and diluted 1:10 in dH_2O prior to assay execution.

4.4. In vivo muscle function

Maximal isometric torque of the plantarflexors was assessed as previously described [54]. Under anesthesia (1% isofluorane in oxygen) mice were placed on a heated stage in the supine position and the right foot was secured to foot-plate attached to a servomotor at 90° relative to the immobilized knee (Model 300C-LR; Aurora Scientific, Ontario, Canada). For nerve stimulated contractions (Nerve Stim); Teflon coated electrodes were inserted percutaneously on either side of the sciatic nerve ~ 1 cm proximal to the knee joint. For direct muscle stimulation (Direct Stim); electrodes were inserted into the proximal and distal ends of the gastrocnemius muscle. Peak isometric torque (mN m), which is referred to as force, was achieved by varying the current delivered to the nerve or muscle and keeping the following parameters constant: 10 V electric potential, 200 Hz stimulation frequency, 300 ms stimulation duration, and 0.3 ms pulse duration. To account for differences in body size among mice, force was normalized by body mass (g), which did not change over the experimental time period. Specific force was calculated by dividing absolute force by plantarflexor wet weight (mg).

4.5. Drug treatment

MitoSNO and MitoNAP, generous gifts from Michael Murphy, were dissolved in 0.9% sterile saline, filtered through 2 μM filter, kept on ice and protected from light immediately

prior to the experiments. Saline, MitoSNO or MitoNAP were injected into the tibialis anterior (100 μL) and GA (150 μL) after 55 min of ischemia.

4.6. Mitotimer analysis

MitoTimer is a mitochondria targeted reporter gene that shifts emission from green (Fitc excitation/emission 488/518 nm) to red (Tritc excitation/emission 543/572 nm) upon oxidation. Mitotimer is a useful tool to measure mitochondrial oxidative stress (red: green ratio) [32,49]. Images were acquired as previously described [32,49]. Briefly, the sciatic nerve (SN) and plantaris muscle (PL) were harvested from the hindlimb and fixed in 4% paraformaldehyde (PFA) for 20 min, washed with phosphate buffered saline (PBS), and mounted on a gelatin coated slide with 50/50 PBS glycerol. Images were acquired via confocal microscopy using Olympus Fluoview FV1000. Quantification of the red: green ratio of plantaris muscle and sciatic nerve using a custom-designed MatLab-based algorithm. For MitoTimer and AchR analysis, plantaris muscle were first prepared as described above then incubated with α-BTX prior to confocal imaging. Analysis of MitoTimer at the NMJ was done manually using ImageJ. All images were acquired with identical acquisition parameters for the respective tissue types.

4.7. NMJ analysis

NMJ area and occupancy were assessed as previously described [2,80]. Briefly, the plantaris muscle was removed and fixed in 4% PFA for 20 min, permeabilized in 3% Triton-X100 in PBS for 30 min and blocked in 1% Triton-X100 + 4% fatty acid-free BSA for 60 min at room temperature. Muscles were then incubated with primary antibodies against Tubulin β-III (Tuj1, Covance 801201) 1:100 and synaptic vesicle 2A (SV2, Abcam ab32942) 1:50 overnight at 4 °C. Muscles were washed 3× with PBS then incubated with Goat-anti-Rabbit-FITC and Goat-anti-Mouse-FITC secondary antibodies for 2 h at RT. Alexa Fluor 647 conjugated α-bungarotoxin (1 μg/mL) (Thermo Scientific B35450) was added to the secondary antibodies after 1.5 h. At the end of 2 h, muscles were rinsed 3× with PBS then mounted on gelatin coated sides using Vectashield (Vector Laboratories H-1000). Images were acquired using Olympus Fluoview FV1000. To assess the whole NMJ, Z-stacks were acquired using both 20× and 60× objectives. Only NMJs completely *en face* acquired at 60× were analyzed. Maximum intensity Z-stacks were reconstructed in ImageJ (National Institutes of Health) and underwent the following corrections in the order listed: background subtraction (50.0 pixels), despeckling, application of a Gaussian blur (2.0 radius) and conversion to binary. Occupancy was determined by dividing the area of the presynaptic structures by the area of post synaptic structures (pre μm^2/post μm^2 × 100). Denervation is defined as the percentage of total NMJs in which the occupancy is > 5%.

4.8. Cryosectioning and staining

Immediately after dissection the plantaris muscle was embedded in a mold filled with Tissue Tek optimal cutting temperature compound then frozen in an isopentane slurry cooled by liquid nitrogen. Transverse sections were cut using a cryostat (5 μm), mounted on positively charged slides, air dried, then stored at −80 °C. Cryosections of plantaris muscle stained with hematoxylin and eosin (H&E) [81] 3 digital images acquired at 20 × magnification and centralized nuclei and fiber number were counted by a blinded investigator. For

immunostaining, slides were removed from the freezer, fixed in 4% PFA for 10 min on ice, then incubated in 0.3% Triton-X100 in PBS for 10 min. After rinsing with PBS sections were circled using a hydrophobic pen and incubated with 5% normal goat serum in PBS for 60 min. Samples were then incubated with primary antibodies against Ncam (Abcam, ab9018) and laminin (Chemicon MAB1928) diluted 1:100 in NGS overnight at 4 °C in a humidified chamber. Samples were washed and incubated with fluorescently conjugated secondary antibodies having been diluted 1:100 in NGS for 60 min at RT. After a 10-min incubation with 7.5 nM 4′,6-diamidino-2-phenylindole (DAPI), and washing with PBS slides were mounted using vectashield and glass coverslips. Images were acquired using Olympus Fluoview FV1000 with identical parameters. The numbers of total fibers and fibers with intracellular staining of Ncam were counted by a blinded investigator.

4.9. Biotin-switch

The biotin switch technique was employed to enrich *S*-nitrosylated proteins in the GA and sciatic nerve as previously described [52]. Briefly, tissues were homogenized in 1:10 mg tissue/mL lysis buffer (50 mM Tris HCL pH 7.5, 1 mM EDTA, 150 mM NaCl, 0.4% triton X-100, 0.1 mM neocuproine + 1 protease inhibitor tablet in 50 mL by 3 strokes at medium speed of polytron. To prove the effectiveness of MitoSNO, we incubated a muscle in vitro with 100 μM MitoSNO with or without 5 mM DTT for 10 min at 37 °C with shaking. Lysate was then centrifuged at 4000 rpm for 15 min at 4 °C and the pellet was discarded. Protein concentration was determined using BCA assay (Pierce) and 100 μg of each sample was placed in 4 volumes of blocking buffer (9 volumes HEN+ 1 vol 25%SDS containing 20 mM MMTS) for 1 h at 55 °C with shaking at 400 rpm. (note: equal concentrations of each sample were saved to serve as input prior to blocking). HEN buffer. Protein was precipitated by adding 2 volumes of ice-cold acetone and placed at −20 °C for 30 min, spun at maximum, and the supernatant was discarded. Protein was suspended in 25 μL of 4 mM HPDP-biotin and 1 μL of 100 mM sodium ascorbate and incubated for 1 h at RT. HPDP-biotin was removed by precipitation with 2 volumes of acetone at −20 °C for 30 min then spun at maximum for 30 min, the supernatant was discarded and the pellet was resuspended in 100 μL HEN buffer (250 mM HEPES pH 7.7, 1 mM EDTA, 0.1 mM neocuproine). Then 200 μL of neutralization buffer (20 mM HEPES pH 7.7, 10 mM NaCl, 1 mM EDTA, 0.5% Triton X-100) and 50 μL streptavidin agarose (Sigma-Aldrich S1638) was added and samples were incubated at RT for 1 h. Samples were then washed 5× with neutralization buffer + 600 mM NaCl. Protein was eluted in 2× sample buffer (80 mM Tris HCl pH 6.8, 2% SDS, 10% glycerol, 0.0006% bromophenol blue, 0.1 M DTT) containing 1 protease inhibitor tablet, 100uL of each phosphatase inhibitors, and equal volumes were loaded to a 10% SDS-Page gel. Following electrophoresis transfer onto a nitrocellulose membrane, and blocking with 5% dried milk, membranes was incubated with Rabbit anti-NDUFS1 (Thermo Scientific PA5-28220) 1:500, a cocktail of mouse primaries against complexes I, II, III, IV, and V of the ETS (abcam ab110413) 1:500, anti-4 Hydroxynonenal (abcam 48506) 1:1000, and Rabbit anti-Actin (sigma A2066) 1:5000.

4.9.1. Mitochondrial isolation—Mitochondria were isolated from sciatic nerve and plantaris muscle as previously described with slight modifications [49]. Tissues were extracted after 3 h of IR and homogenized in fractionation buffer (20 mM HEPES, 250

mM Sucrose, 0.1 mM EDTA, pH 7.4) by 3, 10 s strokes, of a polytron at 40% power (1 mg tissue:10 μL buffer). Immediately after homogenization, samples were centrifuged for 800 × *g* for 10 min at 4 °C. Homogenate was removed, transferred to a new tube, and centrifuged 9000 × *g* for 10 min at 4 °C. resulting pellet was washed in fractionation buffer, centrifuged 9000 × *g* for 10 min at 4 °C and resuspended in 2× sample buffer.

4.10. Statistical analysis

All results are presented as means ± Standard Error of the Mean (SE). One-way analysis of variance was used to compare serum creatine kinase, muscle mass, 14 day maximum specific force, centralized nuclei, NMJ denervation, MitoTimer red: green ratio, mitochondrial content, and network fragmentation. Additionally, since there was no interaction effect between nerve and muscle stimulated force production at day 14 with MitoSNO treatment we performed a 1-way ANOVA comparing treatments. Two-way analysis of variance was used to compare force produced by nerve and muscle stimulation at different time points (stimulation vs. time), and force of nerve and muscle stimulation between treatment groups (stimulation vs. treatment). A significant interaction of 0.05 was required to perform a between-variable post-hoc analysis in which case Tukey's honestly significance difference test was performed.

Supplementary Material

Refer to Web version on PubMed Central for supplementary material.

Acknowledgments

Funding sources

We thank Drs. Mei Lin (Augusta University) and Elizabeth Murphy (National Heart Lung and Blood Instititue, NIH) for the encouragement and insightful discussions. This work was supported by NIH (R01 AR050429) to Z.Y, NIH (T32 HL007284-38) and AHA (114PRE20380254) to R.J.W.

References

1. Pollari E, Goldsteins G, Bart G, Koistinaho J, Giniatullin R. The role of oxidative stress in degeneration of the neuromuscular junction in amyotrophic lateral sclerosis. Front Cell Neurosci. 8 2014; :131. [PubMed: 24860432]
2. Valdez G, Tapia JC, Kang H, Clemenson GD, Gage FH, Lichtman JW, et al. Attenuation of age-related changes in mouse neuromuscular synapses by caloric restriction and exercise. Proc Natl Acad Sci USA. 107 (33) 2010; :14863–14868. [PubMed: 20679195]
3. Pratt SJ, Shah SB, Ward CW, Inacio MP, Stains JP, Lovering RM. Effects of in vivo injury on the neuromuscular junction in healthy and dystrophic muscles. J Physiol. 591 2013; :559–570. [PubMed: 23109110]
4. Kurimoto S, Jung J, Tapadia M, Lengfeld J, Agalliu D, Waterman M, et al. Activation of the Wnt/β-catenin signaling cascade after traumatic nerve injury. Neuroscience. 294 2015; :101–108. [PubMed: 25743255]
5. Carmo-Araújo EM, Dal-Pai-Silva M, Dal-Pai V, Cecchini R, Anjos Ferreira AL. Ischaemia and reperfusion effects on skeletal muscle tissue: morphological and histochemical studies. Int J Exp Pathol. 88 (3) 2007; :147–154. [PubMed: 17504444]
6. Dennis DA, Kittelson AJ, Yang CC, Miner TM, Kim RH, Stevens-Lapsley JE. Does tourniquet use in TKA affect recovery of lower extremity strength and function? A randomized trial. Clin Orthop Relat Res. 474 (1) 2016; :69–77. [PubMed: 26100254]

7. Olivecrona C, Blomfeldt R, Ponzer S, Stanford BR, Nilsson BY. Tourniquet cuff pressure and nerve injury in knee arthroplasty in a bloodless field. Acta Orthop. 84 (2) 2013; :159–164. [PubMed: 23485070]
8. Tömböl T, Pataki G, Németh a, Hamar J. Ultrastructural changes of the neuromuscular junction in reperfusion injury. Cells Tissues Organs. 170 (2–3) 2002; :139–150. [PubMed: 11731702]
9. Eastlack RK, Groppo ER, Hargens AR, Pedowitz RA. Ischemic-preconditioning does not prevent neuromuscular dysfunction after ischemia – reperfusion injury. J Orthop Res. 22 (4) 2004; :918–923. [PubMed: 15183455]
10. Duehrkop C, Rieben R. Refinement of tourniquet-induced peripheral ischemia/ reperfusion injury in rats: comparison of 2 h vs 24 h reperfusion. Lab Anim. 48 (2) 2014; :143–154. [PubMed: 24585935]
11. Teng D, Hornberger TA. Optimal temperature for hypothermia intervention in mouse model of skeletal muscle ischemia reperfusion injury. Cell Mol Bioeng. 4 (4) 2011; :717–723.
12. Lysakowski A, Figueras H, Price SD, Peng Y. Dense-cored vesicles, smooth endoplasmic reticulum, and mitochondria are closely associated with non-specialized parts of plasma membrane of nerve terminals: implications for exocytosis and calcium buffering by intraterminal organelles. J Comp Neurol. 390 (1998) 1999; :378–390.
13. Wong M, Martin LJ. Skeletal muscle-restricted expression of human SOD1 causes motor neuron degeneration in transgenic mice. Hum Mol Genet. 19 (11) 2010; :2284–2302. [PubMed: 20223753]
14. Alnaes E, Rahamimoff R. On the role of mitochondria in transmitter release from motor nerve terminals. J Physiol. 248 (2) 1975; :285–306. [PubMed: 50439]
15. Verstreken P, Ly CV, Venken KJT, Koh TW, Zhou Y, Bellen HJ. Synaptic mitochondria are critical for mobilization of reserve pool vesicles at Drosophila neuromuscular junctions. Neuron. 47 (3) 2005; :365–378. [PubMed: 16055061]
16. Hollenbeck PJ. Mitochondria and neurotransmission: evacuating the synapse. Neuron. 47 (3) 2005; :331–333. [PubMed: 16055057]
17. O'Hanlon GM, Humphreys PD, Goldman RS, Halstead SK, Bullens RWM, Plomp JJ, et al. Calpain inhibitors protect against axonal degeneration in a model of antiganglioside antibody-mediated motor nerve terminal injury. Brain. 126 (11) 2003; :2497–2509. [PubMed: 12937083]
18. Lejay A, Meyer A, Schlagowski A-I, Charles A-L, Singh F, Bouitbir J, et al. Mitochondria: mitochondrial participation in ischemia-reperfusion injury in skeletal muscle. Int J Biochem Cell Biol. 50 2014; :101–105. [PubMed: 24582887]
19. Tran TP, Tu H, Liu J, Muelleman RL, Li Y-L. Mitochondria-derived superoxide links to tourniquet-induced apoptosis in mouse skeletal muscle. PLoS One. 7 (8) 2012; :e43410. [PubMed: 22912870]
20. Fillingame RH, Coupling H. transport and ATP synthesis in F1F0-ATP synthases: glimpses of interacting parts in a dynamic molecular machine. J Exp Biol. 200 (2) 1997; :217–224. [PubMed: 9050229]
21. Murphy MP. How mitochondria produce reactive oxygen species. Biochem J. 417 (1) 2009; :1–13. [PubMed: 19061483]
22. Loschen G, Azzi A, Richter C, Plohi L. Superoxide radicals as precursors of mitochondrial hydrogen peroxide. FEBS Lett. 42 (1) 1974; :68–72. [PubMed: 4859511]
23. Handy DE, Loscalzo J. Redox regulation of mitochondrial function. Antioxid Redox Signal. 16 (11) 2012; :1323–1367. [PubMed: 22146081]
24. Chen Q, Camara AKS, Stowe DF, Hoppel CL, Lesnefsky EJ. Modulation of electron transport protects cardiac mitochondria and decreases myocardial injury during ischemia and reperfusion. AJP Cell Physiol. 292 (1) 2006; :C137–C147.
25. Chouchani ET, Pell VR, Gaude E, Aksentijević D, Sundier SY, Robb EL, et al. Ischaemic accumulation of succinate controls reperfusion injury through mitochondrial ROS. Nature. 515 (7527) 2014; :431–435. [PubMed: 25383517]
26. Neely JR, Grotyohann LW. Role of glycolytic products in damage to ischemic myocardium. Dissociation of adenosine triphosphate levels and recovery of function of reperfused ischemic hearts. Circ Res. 55 (6) 1984; :816–824. [PubMed: 6499136]

27. Dröse S, Brandt U, Wittig I. Mitochondrial respiratory chain complexes as sources and targets of thiol-based redox-regulation. Biochim Biophys Acta. 2014
28. Tran TP, Tu H, Pipinos II, Muelleman RL, Albadawi H, Li Y-L. Tourniquet-induced acute ischemia-reperfusion injury in mouse skeletal muscles: involvement of superoxide. Eur J Pharmacol. 650 (1) 2011; :328–334. [PubMed: 21036124]
29. Näpänkangas JP, Liimatta EV, Joensuu P, Bergmann U, Ylitalo K, Hassinen IE. Superoxide production during ischemia-reperfusion in the perfused rat heart: a comparison of two methods of measurement. J Mol Cell Cardiol. 53 (6) 2012; :906–915. [PubMed: 23036824]
30. Sheu SS, Nauduri D, Anders MW. Targeting antioxidants to mitochondria: a new therapeutic direction. Biochim Biophys Acta - Mol Basis Dis. 1762 (2) 2006; :256–265.
31. Nichenko, AS; Southern, WM; Atuan, M; Luan, J; Peissig, KB; Foltz, SJ; , et al. Mitochondrial maintenance via autophagy contributes to functional skeletal muscle regeneration and remodeling. Am J Physiol Cell Physiol. 2016.
32. Laker RC, Xu P, Ryall Ka, Sujkowski A, Kenwood BM, Chain KH, et al. A novel MitoTimer reporter gene for mitochondrial content, structure, stress, and damage in vivo. J Biol Chem. 289 (17) 2014; :12005–12015. [PubMed: 24644293]
33. Sun J, Murphy E. Protein S-nitrosylation and cardioprotection. Circ Res. 106 (2) 2010; :285–296. [PubMed: 20133913]
34. Chen YY, Chu HM, Pan KT, Teng CH, Wang DL, Wang AHJ, et al. Cysteine S-nitrosylation protects protein-tyrosine phosphatase 1B against oxidation-induced permanent inactivation. J Biol Chem. 283 (50) 2008; :35265–35272. [PubMed: 18840608]
35. Chang AHK, Sancheti H, Garcia J, Kaplowitz N, Cadenas E, Han D. Respiratory substrates regulate S-nitrosylation of mitochondrial proteins through a thiol-dependent pathway. Chem Res Toxicol. 27 (5) 2014; :794–804. [PubMed: 24716714]
36. Sun J, Morgan M, Shen R-F, Steenbergen C, Murphy E. Preconditioning results in S-nitrosylation of proteins involved in regulation of mitochondrial energetics and calcium transport. Circ Res. 101 (11) 2007; :1155–1163. [PubMed: 17916778]
37. Sasaki N, Sato T, Ohler a, O'Rourke B, Marbán E. Activation of mitochondrial ATP-dependent potassium channels by nitric oxide. Circulation. 101 (4) 2000; :439–445. [PubMed: 10653837]
38. Chouchani ET, Methner C, Nadtochiy SM, Logan A, Pell VR, Ding S, et al. Cardioprotection by S-nitrosation of a cysteine switch on mitochondrial complex I. Nat Med. 19 (6) 2013; :753–759. [PubMed: 23708290]
39. Prime, Ta; Blaikie, FH; Evans, C; Nadtochiy, SM; James, AM; Dahm, CC; , et al. A mitochondria-targeted S-nitrosothiol modulates respiration, nitrosates thiols, and protects against ischemia-reperfusion injury. Proc Natl Acad Sci USA. 106 (26) 2009; :10764–10769. [PubMed: 19528654]
40. Ingram TE, Fraser AG, Bleasdale Ra, Ellins Ea, Margulescu AD, Halcox JP, et al. Low-dose sodium nitrite attenuates myocardial ischemia and vascular ischemia-reperfusion injury in human models. J Am Coll Cardiol. 61 (25) 2013; :2534–2541. [PubMed: 23623914]
41. Standards of practice for safe use of pneumatic tourniquet [Internet]. Association of Surgical Technologies; 2007. Available from: <http://www.ast.org/uploadedFiles/Main_Site/Content/About_Us/StandardsPneumaticTourniquets.pdf>
42. Walters, TJ, Wenke, JC, Baer, DA. Research on Tourniquet Related Injury for Combat Casualty Care. Aug, 2004 8–16.
43. Apple FS, Rhodes M. Enzymatic estimation of skeletal muscle damage by analysis of changes in serum creatine kinase. J Appl Physiol. 65 (6) 1988; :2598–2600. [PubMed: 3215860]
44. Brancaccio P, Maffulli N, Limongelli FM. Creatine kinase monitoring in sport medicine. Br Med Bull. 2007 :209–230. [PubMed: 17569697]
45. Karalaki M, Fili S, Philippou A, Koutsilieris M. Muscle regeneration: cellular and molecular events. Vivo. 23 (5) 2009; :779–796.
46. Hirsch NP. Neuromuscular junction in health and disease. Br J Anaesth. 99 (1) 2007; :132–138. [PubMed: 17573397]
47. Nishizawa T, Tamaki H, Kasuga N, Takekura H. Degeneration and regeneration of neuromuscular junction architecture in rat skeletal muscle fibers damaged by bupivacaine hydrochloride. J Muscle Res Cell Motil. 24 (8) 2003; :527–537. [PubMed: 14870968]

48. Wilson RJ, Drake JC, Cui D, Zhang M, Perry HM, Kashatus JA, et al. Conditional MitoTimer reporter mice for assessment of mitochondrial structure, oxidative stress, and mitophagy. Mitochondrion. 2017
49. Laker RC, Drake JC, Wilson RJ, Lira VA, Lewellen BM, Ryall KA, et al. Ampk phosphorylation of Ulk1 is required for targeting of mitochondria to lysosomes in exercise-induced mitophagy. Nat Commun. 8 (1) 2017; :548. [PubMed: 28916822]
50. Kohr MJ, Sun J, Aponte A, Wang G, Gucek M, Murphy E, et al. Simultaneous measurement of protein oxidation and S-nitrosylation during preconditioning and ischemia/reperfusion injury with resin-assisted capture. Circ Res. 108 (4) 2011; :418–426. [PubMed: 21193739]
51. Schoen M, Rotter R, Gierer P, Gradl G, Strauss U, Jonas L, et al. Ischemic preconditioning prevents skeletal muscle tissue injury, but not nerve lesion upon tourniquet-induced ischemia. J Trauma. 63 (4) 2007; :788–797. [PubMed: 18090007]
52. Jaffrey SR, Snyder SH. The biotin switch method for the detection of S-nitrosylated proteins. Sci STKE. 2001 (86) 2001; :pl1.
53. Gillon A, Sheard P. Elderly mouse skeletal muscle fibres have a diminished capacity to upregulate NCAM production in response to denervation. Biogerontology. 16 (6) 2015; :811–823. [PubMed: 26385499]
54. Call, JA; Wilson, RJ; Laker, RC; Zhang, M; Kundu, M; Yan, Z. Ulk1-mediated autophagy plays an essential role in mitochondrial remodeling and functional regeneration of skeletal muscle; Am J Physiol – Cell Physiol. 2017. 4477
55. Mech LD. Common pathway for the red chromophore formation in fluorescent proteins and chromoproteins. Can Field-Nat. 128 (2) 2014; :189–190.
56. Jang YC, Lustgarten MS, Liu Y, Muller FL, Bhattacharya A, Liang H, et al. Increased superoxide in vivo accelerates age-associated muscle atrophy through mitochondrial dysfunction and neuromuscular junction degeneration. FASEB J. 24 (5) 2010; :1376–1390. [PubMed: 20040516]
57. Aktaş E, Atay Ç, Deveci MA, Arikan M, Toğral G, Yildirim A. Impact of oxidative stress on early postoperative knee function and muscle injury biochemical markers: is it possible to create an ischemic preconditioning effect in sequential ischemic surgical procedures? Acta Orthop Traumatol Turc. 49 (4) 2015; :387–393. [PubMed: 26312465]
58. Brini M, Marsault R, Bastianutto C, Alvarez J, Pozzan T, Rizzuto R. Transfected aequorin in the measurement of cytosolic Ca^{2+} concentration ($[Ca^{2+}](c)$). A critical evaluation. J Biol Chem. 270 1995; :9896–9903. [PubMed: 7730373]
59. Chang DTW, Reynolds IJ. Differences in mitochondrial movement and morphology in young and mature primary cortical neurons in culture. Neuroscience. 141 (2) 2006; :727–736. [PubMed: 16797853]
60. Kalogeris T, Baines C. Cell biology of ischemia/reperfusion injury. Int Rev Cell Mol Biol Mol Biol. 298 2012; :229–317.
61. Li N, Brun T, Cnop M, Cunha DA, Eizirik DL, Maechler P. Transient oxidative stress damages mitochondrial machinery inducing persistent β-cell dysfunction. J Biol Chem. 284 (35) 2009; :23602–23612. [PubMed: 19546218]
62. Piantadosi CA. Regulation of mitochondrial processes by protein S-nitrosylation. Biochim Biophys Acta. 1820 (6) 2012; :712–721. [PubMed: 21397666]
67. Kohr MJ, Sun J, Aponte A, Wang G, Gucek M, Murphy E, et al. Simultaneous measurement of protein oxidation and S-nitrosylation during preconditioning and ischemia/reperfusion injury with resin-assisted capture. Circ Res. 108 (4) 2011; :418–426. [PubMed: 21193739]
68. Kumar A, Kaundal RK, Iyer S, Sharma SS. Effects of resveratrol on nerve functions, oxidative stress and DNA fragmentation in experimental diabetic neuropathy. Life Sci. 80 (13) 2007; :1236–1244. [PubMed: 17289084]
69. Crow JP, Calingasan NY, Chen J, Hill JL, Beal MF. Manganese porphyrin given at symptom onset markedly extends survival of ALS mice. Ann Neurol. 58 (2) 2005; :258–265. [PubMed: 16049935]
70. Dorion D, Zhong A, Chiu C, Forrest CR, Boyd B, Pang CY. Role of xanthine oxidase in reperfusion injury of ischemic skeletal muscles in the pig and human. J Appl Physiol. 75 (1) 1993; :246–255. [PubMed: 8397177]

71. Stupka N, Tiidus PM. Effects of ovariectomy and estrogen on ischemia-reperfusion injury in hindlimbs of female rats. J Appl Physiol. 91 (4) 2001; :1828–1835. [PubMed: 11568169]
72. Gillani S, Cao J, Suzuki T, Hak DJ. The effect of ischemia reperfusion injury on skeletal muscle. Injury. 43 (6) 2012; :670–675. [PubMed: 21481870]
73. Fink E, Fortin D, Serrurier B, Ventura-Clapier R, Bigard AX. Recovery of contractile and metabolic phenotypes in regenerating slow muscle after notexin-induced or crush injury. J Muscle Res Cell Motil. 24 (7) 2003; :421–429. [PubMed: 14677645]
74. Pintér S, Mendler L, Dux L. Neural impacts on the regeneration of skeletal muscles. Acta Biochim Pol. 50 (4) 2003; :1229–1237. [PubMed: 14740009]
75. Kraft GH. Fibrillation potential amplitude and muscle atrophy following peripheral nerve injury. Muscle Nerve. 13 (9) 1990; :814–821. [PubMed: 2233867]
76. Leterme D, Tyc F. Re-innervation and recovery of rat soleus muscle and motor unit function after nerve crush. Exp Physiol. 89 (4) 2004; :353–361. [PubMed: 15123555]
77. Gorman CM, Moffat LF, Howard BH. Recombinant genomes which express chloramphenicol acetyltransferase in mammalian cells. Mol Cell Biol. 2 (9) 1982; :1044–1051. [PubMed: 6960240]
78. Alexopoulou AN, Couchman JR, Whiteford JR. The CMV early enhancer/ chicken β actin (CAG) promoter can be used to drive transgene expression during the differentiation of murine embryonic stem cells into vascular progenitors. BMC Cell Biol. 9 (1) 2008; :2. [PubMed: 18190688]
79. Bonheur, Ja; Albadawi, H; Patton, GM; Watkins, MT. A noninvasive murine model of hind limb ischemia-reperfusion injury. J Surg Res. 116 (1) 2004; :55–63. [PubMed: 14732349]
80. Pratt SJP, Shah SB, Ward CW, Kerr JP, Stains JP, Lovering RM. Recovery of altered neuromuscular junction morphology and muscle function in mdx mice after injury. Cell Mol Life Sci. 72 (1) 2014; :153–164. [PubMed: 24947322]
81. Mufti SA, Carlson BM, Maxwell LC, Faulkner JA. The free autografting of entire limb muscles in the cat: morphology. Anat Rec. 188 (4) 1977; :417–429. [PubMed: 900525]

Appendix A. Supplementary material

Supplementary data associated with this article can be found in the online version at http://dx.doi.org/10.1016/j.freeradbiomed.2018.02.006.

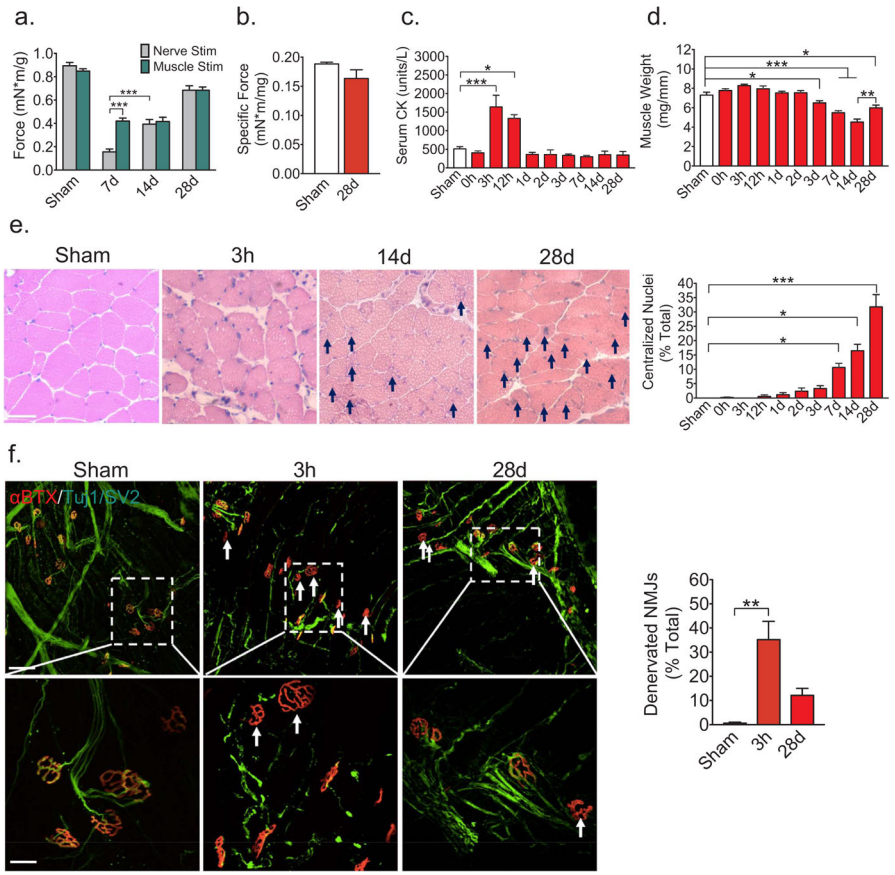

Fig. 1. Tourniquet-induced IR in skeletal muscle causes both nerve and muscle damages

To determine the consequence of IR on skeletal muscle and motor nerve fibers a rubber band was applied to induce ischemia and released after 1 h to initiate reperfusion. Muscle function and muscle injury as well as motor nerve innervation were assessed at indicated time points over 28 days. (a) Comparison of tetanic force production of plantar flexors by nerve stimulation or muscle stimulation after IR at multiple time points (** and *** denote $p < 0.01$ and $p < 0.001$, respectively, n = 6). Other statistically significant comparisons are presented in Supplemental Table 1; (b) Specific tetanic force 28 days following injury; (c) Serum creatine kinase activity (* and *** denote $p < 0.05$ and $p < 0.001$, respectively, n = 3–5); (d) Wet weight of GA muscle normalized by tibia length (mm). (*, ** and *** denote $p < 0.05$, $p < 0.01$ and $p < 0.001$, respectively, n = 6–8); (e) Representative light microscope images of H&E stained skeletal muscle cross sections and percentage of fibers with centralized nuclei (scale bar = 100 μm, * and *** denote $p < 0.05$ and $p < 0.001$, respectively, n = 3–5); (f) Representative confocal images of α-bungarotoxin (α-BTX, red) and beta III-tubulin/synaptic vesicle protein-2 (Tuj1/SV2, green) and percentage of denervated NMJ following IR (scale bar = 50 μm and 20 μm for the top panel and bottom enlarged panel, respectively, ** denotes $p < 0.01$, n = 5–7). Data are represented as mean ± SEM.

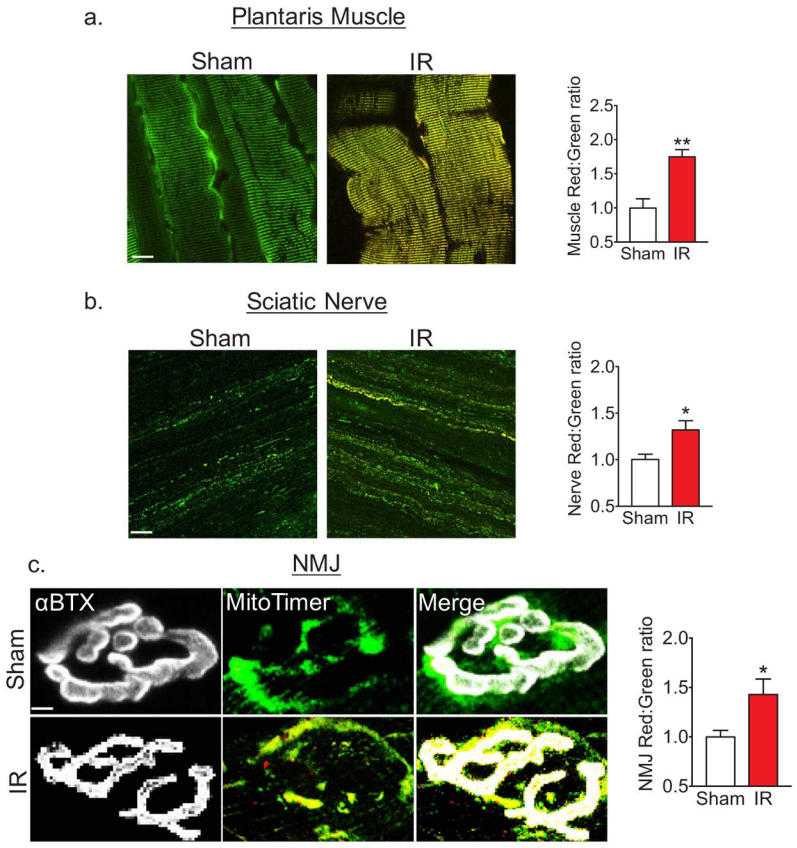

Fig. 2. Ischemia-reperfusion causes mitochondrial oxidative stress in skeletal muscle, motor nerve, and NMJ

To determine the impact of IR on mitochondrial oxidative stress *MitoTimer* transgenic mice were subjected to IR followed by 3 h of reperfusion. Representative confocal images and quantification of MitoTimer red:green in (a) plantaris muscle and (b) sciatic nerve (scale bar = 50 μm, * and ** denote $p < 0.05$ and $p < 0.01$, respectively, n = 3–4); (c) Representative images of α-BTX (gray) and MitoTimer (green and red) colocalization with NMJ and quantification of MitoTimer red:green ratio at the NMJ (scale bar = 5 μm, * denotes $p < 0.05$, n = 3). Data are represented as mean ± SEM.

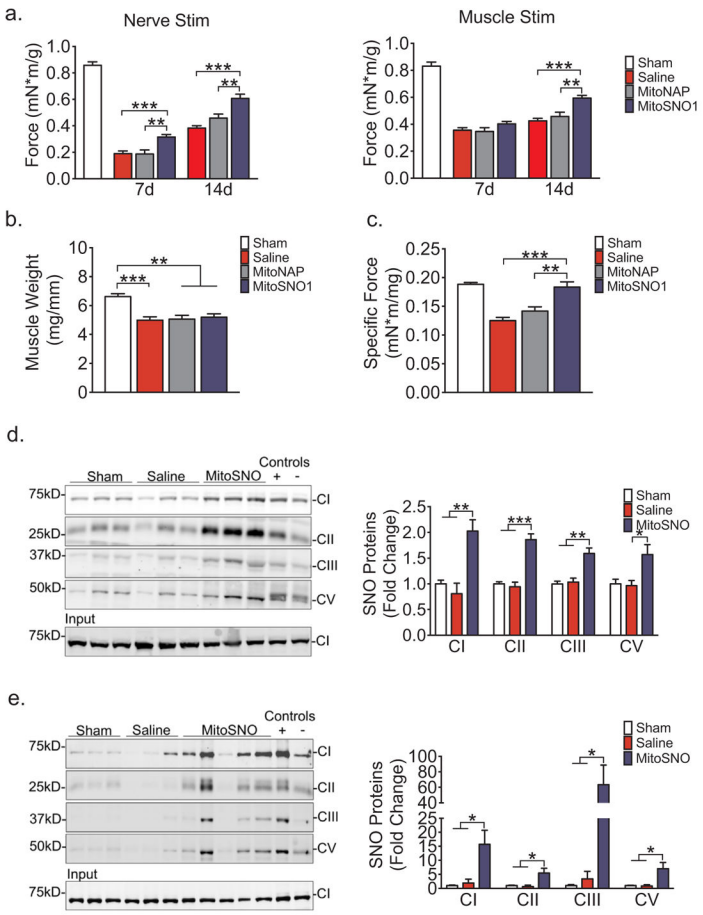

Fig. 3. MitoSNO preserves neuromuscular function and facilitates recovery of muscle force

To determine whether enhancement of mitochondrial protein SNO could attenuate IR injury to the nerve and/or skeletal muscle, saline, MitoSNO or MitoNAP were injected intramuscularly to ischemic muscle 5 min prior to the release of the tourniquet. Mitochondrial protein SNO, nerve and muscle function, and muscle mass were measured at indicated time points. (a) Maximum tetanic force produced by nerve stimulation or muscle stimulation at days 7 and 14 following IR (** and *** denote $p < 0.01$ and $p < 0.001$, respectively, n = 6–9); (b) Mass of gastrocnemius muscle at day 14 normalized to tibia length (mm) (*** denotes $p < 0.001$, n = 6); (c) Nerve-stimulated specific force at day 14 (*** denotes $p < 0.001$, n = 6). Immunoblots and quantification of complexes I, II, III and V of the ETS from (d) gastrocnemius muscle (e) and sciatic nerve following biotin switch assay. Control of SNO reaction was provided by incubation of tissues in vitro with either MitoSNO or MitoSNO + Dithiothreitol. (*, **, and ***, denote $p < 0.05$, $p < 0.01$, and $p < 0.001$, respectively, n = 3–5). Data are represented as mean ± SEM.

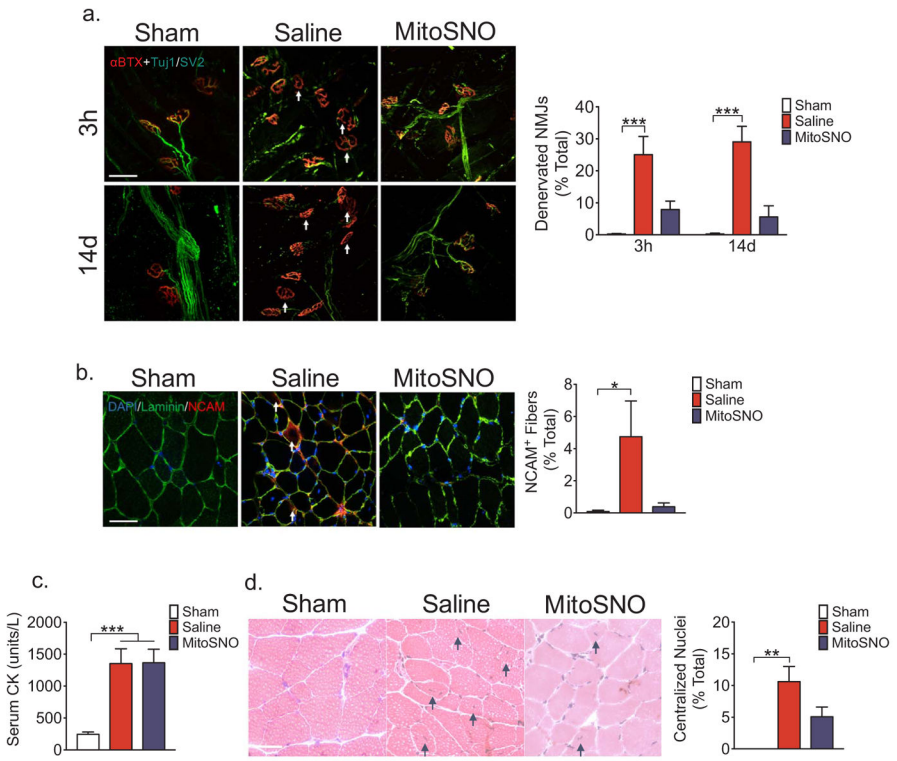

Fig. 4. MitoSNO attenuates denervation of NMJ

To elucidate the consequence of MitoSNO treatment on NMJ innervation and muscle injury we subjected ischemic hindlimb muscle to saline or MitoSNO treatment prior to release tourniquet for reperfusion. with sham treated mice as control. (a) Representative confocal images and quantification of percentage of denervated NMJs 3 h and 14 days following IR (scale bar = 20 μm, *** denotes $p < 0.001$, n = 5–6); (b) Representative confocal images of transverse sections of skeletal muscle expressing Ncam (red), Laminin (green), and DAPI (blue) and quantification of the percentage Ncam positive fibers at 14 days following injury (scale bar = 100 μm, * denotes $p < 0.05$, n = 4); (c) Serum creatine kinase activity 3 h following IR (*** denotes $p < 0.001$, n = 6); (d) Representative images of H&E stained transverse sections of skeletal muscle and quantification of percentage of fibers with centralized nuclei 14 days following IR (scale bar = 50 μm, ** denotes $p < 0.01$, n = 4). Data are represented as mean ± SEM.

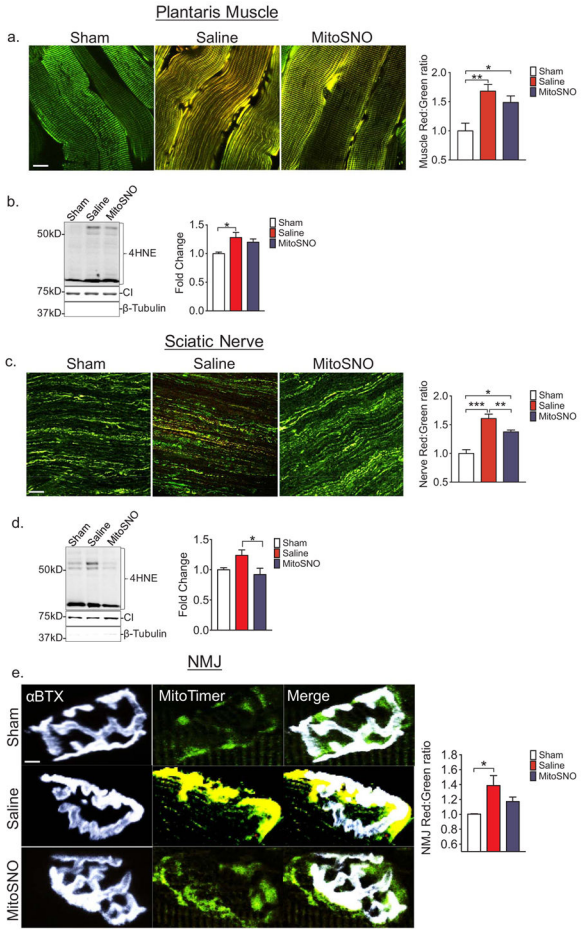

Fig. 5. MitoSNO reduces IR-induced mitochondrial oxidative stress in the motor nerve

To determine the effect(s) of MitoSNO treatment on mitochondria oxidative stress in the motor nerve and skeletal muscle fibers, we assessed MitoTimer red:-green via confocal microscopy and 4HNE in isolated mitochondria from the plantaris muscle and sciatic nerve 3 h following injury. (a) Representative confocal images and quantification of Mitotimer red:-green ratio of plantaris muscle (scale bar = 50 μm, * and ** denote $p < 0.05$ and $p < 0.01$, respectively, n = 7); (b) Representative immunoblot and quantification of 4HNE in mitochondria isolated from plantaris muscle (* denotes $p < 0.05$, n = 6); (c) Representative confocal images and quantification of Mitotimer red:green ratio of sciatic nerve (scale bar = 50 μm, *, **, and *** denote $p < 0.05$, $p < 0.01$, and $p < 0.001$, respectively, n = 7), (d) Representative immunoblot and quantification of 4HNE in mitochondria isolated from sciatic nerve (* denotes $p < 0.05$, n = 3); (e) Representative images of α-BTX (gray) and MitoTimer (green and red) co-localization with NMJ and quantification of MitoTimer red:green ratio at the NMJ (scale bar = 5 μm, * denotes $p < 0.05$, n = 4). Data are represented as mean ± SEM.